Induced Fit in Arginine Kinase

Genfa Zhou,* W. Ross Ellington,*† and Michael S. Chapman*‡
‡Department of Chemistry, †Department of Biological Sciences, and *Institute of Molecular Biophysics, Florida State University, Tallahassee, Florida 32306-4380, USA

ABSTRACT Creatine kinase (CK) and arginine kinase (AK) are related enzymes that reversibly transfer a phosphoryl group between a guanidino compound and ADP. In the buffering of ATP energy levels, they are central to energy metabolism and have been paradigms of classical enzymology. Comparison of the open substrate-free structure of CK and the closed substrate-bound structure of AK reveals differences that are consistent with prior biophysical evidence of substrate-induced conformational changes. Large and small domains undergo a hinged 13° rotation. Several loops become ordered and adopt different positions in the presence of substrate, including one (residues 309–319) that moves 15 Å to fold over the substrates. The conformational changes appear to be necessary in aligning the two substrates for catalysis, in configuring the active site only when productive phosphoryl transfer is possible, and excluding water from the active site to avoid wasteful ATP hydrolysis.

INTRODUCTION

Phosphagen kinases are a family of enzymes that include creatine kinase (CK) in vertebrates and arginine kinase (AK) in arthropods and other invertebrates (Kenyon and Reed, 1983; Strong and Ellington, 1993). Their function is to catalyze the reversible transfer of a phosphoryl group between a phosphorylated guanidino (phosphagen) compound and adenosine diphosphate (ADP). These enzymes play a central role in cellular energy metabolism with the temporal buffering of ATP levels in cells with fluctuating energy requirements (muscle, nerves, etc.) and in shuttling energy between difference cellular compartments (Wallimann et al., 1992). These enzymes are also paradigms for the classical enzymology of bimolecular reactions that, from a structural perspective, are less well characterized than their unimolecular counterparts (Stroud, 1996).

This work is based on two phosphagen kinase structures that have been determined recently: 1) an octameric vertebrate mitochondrial creatine kinase (Mi_b-CK) in the *apo* form or as a binary complex with ATP (but not Mg^{2+}), both at ~3 Å resolution (Fritz-Wolf et al., 1996); and 2) a monomeric arthropod arginine kinase (AK) crystallized as a transition state analog (TSA) complex with Mg^{2+}ADP, nitrate (mimicking a planar phosphoryl in transition), and arginine (Zhou et al., 1998), and determined at 1.86-Å resolution. These structures are the fruits of extensive efforts in many laboratories over a period of 30 years, and, although other *apo* structures have since been determined (Rao et al., 1998), there is still no sign that it will be possible to crystallize creatine kinase in an active configuration (Kabsch and Fritz-Wolf, 1997). Thus we turn to a comparison between two different members of the family to understand the conformational changes occurring on substrate binding. This is not ideal, because there are other possible causes of conformational differences (detailed below), but there is extensive independent biophysical evidence (see below) consistent with the assertion that the observed structural differences reflect substrate-induced conformational changes in both enzymes.

Phosphagen kinases share a common mechanism of direct, in-line γ-phosphoryl transfer (Hansen and Knowles, 1981). The transition state structure of AK led to a substantially different understanding of the catalytic mechanism (Zhou et al., 1998) in which substrate alignment appeared to be more important than other mechanisms, such as acid-base catalysis. The direct visualization of precise prealignment of substrates in any enzyme was of general interest, because it had been predicted to be a significant contributor to the catalysis of many bimolecular reactions, either through reduction of the entropic component to the activation barrier (Page and Jencks, 1971), or through alignment of the reactant orbitals on the optimal trajectory (Dafforn and Koshland, 1971). The focus of this report is not the details of catalysis, but the implications of differences between the two structures in terms of the function of these enzymes.

Creatine and arginine are examples of a family of substrates used by different phosphagen kinases. The substrates differ in size and chemical properties, but all share a reactive guanidinium group. The phosphagen kinases share ~40% amino acid identity (Babbitt et al., 1986; Dumas and Camonis, 1993; Mühlebach et al., 1994; Suzuki and Furukohri, 1994), and except in cases where there is evidence of gene duplication (Stein et al., 1990; Suzuki et al., 1997a) or triplication (Wothe et al., 1990), most have subunit molecular masses of ~40 kDa. Although the core part of the structure appears to be conserved, particular enzymes and isoforms have some side distinctive characters. For exam-

Received for publication 28 June 1999 and in final form 30 November 1999.

Address reprint requests to Dr. Michael S. Chapman, Institute of Molecular Biophysics, Florida State University, Tallahassee, FL 32306-4380. Tel.: 850-644-8354; Fax: 850-561-1406. E-mail: chapman@sb.fsu.

0006-3495/00/03/1541/10 $2.00

ple, unlike AK, Mi_b-CK has a C-terminal region of 17 amino acids that is thought to mediate an adhesion between inner and outer mitochondrial membranes via electrostatic interactions (Rojo et al., 1991). Mi_b-CK octamers are functionally and perhaps physically coupled to ATP/ADP translocators of the inner mitochondrial membrane (Wyss et al., 1992). Thus it is possible that some of the surface differences between the two structures are due to specializations relevant to different quaternary structure, intracellular compartmentalization, and possibly function. However, there is much evidence, detailed below, that conformational changes are directly involved in catalysis and that the mechanism is shared by all phosphagen kinases. Furthermore, x-ray small-angle scattering shows that it is the combination of Mg^{2+} + ADP or ATP (substrates common to all phosphagen kinases) that elicits the conformational change and not the phosphagen (creatine, arginine, etc.) that is specific for each enzyme (Forstner et al., 1998).

Prior evidence of substrate-induced conformational changes in both AK and CK include spectroscopic studies of the active site (Reed and Cohn, 1972), tryptic susceptibility differences (Lui and Cunningham, 1966), and x-ray solution scattering (Dumas and Janin, 1983; Forstner et al., 1996, 1998). The conformational changes are induced by the presence of MgATP or the full set of transition state analog (TSA) components—Mg^{2+}, ADP, nitrate (mimicking a phosphoryl group in transfer), and creatine (or arginine)—but not by ATP alone. The *apo*-enzyme is considered to be in "open" form, changing to "closed" when the substrates bind (Forstner et al., 1998). Although differences in the x-ray scattering indicate substantial changes, circular dichroism and sedimentation indicate that the secondary and quaternary structures of Mi_b-CK are unchanged (Forstner et al., 1996). NMR spectroscopy indicates that the chemistry of the reaction is not rate limiting (Rao et al., 1976). This leaves open the possibility that all or part of the conformational change occurs on each reaction cycle and is rate limiting. AK's catalytic turnover ($k_{cat} \approx 135\ s^{-1}$) (Blethen, 1972) is at the slow end of those measured for enzymes (1 to $10^7\ s^{-1}$) (Boyer, 1998), as are others undergoing substrate-induced conformational changes, such as tryptophan synthetase ($2\ s^{-1}$) and lactate dehydrogenase ($1000\ s^{-1}$) (Rhee et al., 1997; Gerstein and Chothia, 1991; Boyer, 1998).

The substrate-induced conformational changes that have been reported in several other systems are manifested as two kinds of motion:

1. *Domain movements*: Yeast hexokinase gave us the first structural paradigm for induced fit. The active site is located in a cleft between two globular domains that closes upon substrate binding (Bennett and Steitz, 1980). Similar mechanisms were proposed for other kinases (Anderson et al., 1979).

2. *Loop movements*: In other enzymes, a flexible loop folds over the active site after substrate binding. Paradigms of this type of change include triosephosphate isomerase (Alber et al., 1987) and RuBisCo (Schreuder et al., 1993), in which the catalytic Lys^{334} follows the substrate with a movement of 13 Å to complete the active site. Substrate-induced conformational changes can be important in allosteric control mechanisms. However, it has been pointed out that induced fit is potentially disadvantageous, especially for nonallosteric enzymes, because the energy required to make the protein conformational change adds to the enthalpy of the activation barrier and reduces catalysis (Fersht, 1985). This perhaps accounts for the rarity of large structural changes during catalysis and for the relatively low energy barrier to such changes when they do accompany catalysis (Gerstein et al., 1994). In the examples given, it appears that the energy-consuming conformational changes are a necessary cost of excluding water from the active site to stop an unwanted side reaction. The phosphagen kinases may be like other kinases (Anderson et al., 1979) in needing to exclude water to avoid the waste of energy with free (solvent-mediated) hydrolysis of ATP.

In this report, differences between the TSA complex (TSAC) AK structure and those of the *apo* Mi_b-CK structure are analyzed for their implications upon the conformational changes between open and closed forms of phosphagen kinases. They suggest that substrate binding induces a 13° domain rotation and large loop conformational changes that reconfigure critical elements of the active site and close the active site to exterior solvent during the reaction.

MATERIALS AND METHODS

Coordinates and alignment

The TSAC-AK coordinates were as described by Zhou et al. (1998) (PDB entry 1bg0). For alignment purposes, the small domain was defined as residues 2–99 (Met^1 is disordered) and the large (C-terminal) domain as residues 100–357. For CK, most of the comparisons were made with the *apo*-enzyme (Fritz-Wolf et al., 1996) (PDB entry 1crk). The small domain was defined as residues 1–102 and the large domain as residues 103–363. The C-terminal fragment 364–380 is unique to Mi_b-CK and is thought to be associated with membrane attachment. The four subunits in the Mi_b-CK asymmetrical unit have slightly different conformations in the flexible N-terminal loop and disordered loop 315–325. Subunit A was used for alignment and structural comparisons.

An approximate transformation for superimposing the CK structure on AK was available from the cross-rotation and translation functions calculated from the AK diffraction amplitudes and CK coordinates during the AK structure determination (Zhou et al., 1999). This was used to improve the pairing of AK and CK amino acids beyond that available from prior sequence alignments (Dumas and Camonis, 1993; Strong and Ellington, 1995). The alignment was least-squares optimized, using O (Jones and Kjeldgaard, 1997) and Lsqkab (Kabsch, 1976) as implemented in the CCP4 suite (Collaborative Computational Project, 1994). Domains were aligned independently. Details of how the transformations were defined are provided in Table 1.

TABLE 1 Transformations to superimpose the coordinates of apo-Mi_b-CK ($\vec{x}_{aCK}$; Fritz-Wolf et al., 1996) on AK ($\vec{x}_{AK}$; Zhou et al., 1998)

Superimposition of whole subunit to optimize alignment of large domain					
Rotation matrix (R_L)				Translation vector (t_L)	
	0.159	0.514	−0.843	8.460	
	0.920	0.232	0.315	−37.363	
	0.358	−0.826	−0.436	60.742	
Subsequent optimization of small domain alignment					
Rotation matrix (R_S)				Translation vector (t_S)	Origin (o)
	0.982	0.116	0.147	−4.333	15.367
	−0.096	0.986	−0.138	7.011	−9.876
	−0.160	0.121	0.980	4.368	40.150
Magnitude 13.0°				0.234 Å	
Axis direction cosines	0.570	0.676	−0.466		

As single rigid bodies, the proteins were first superimposed by a transformation ($\vec{x}'_{aCK} = [R_L]\vec{x}_{aCK} + \vec{t}_L$, where R is a rotation matrix and t is a translation vector) that optimized the agreement in the large domain (L). (The translation vector of such an operation can be considered to be a combination of a real translation and a change in the position of an arbitrary origin.) The small domain (S) of the transformed Mi_b-CK was then further transformed by an operation to optimally align the small domain, in which the arbitrary origin shifts (o) were explicitly factored to give the smallest magnitude translation vector, $\vec{t}_S$: ${}_s\vec{x}''_{aCK} = [R_S]({}_s\vec{x}'_{aCK} - \vec{o}) + \vec{t}_S + \vec{o}$.

Modeling the open state of AK and calculation of radii of gyration

Radii of gyration were calculated from the atomic coordinates following the method of McDonald et al. (1979):

$$R_G = \left(\sum_i Z_i(\vec{x}_i - \vec{m})^2 \Big/ \sum_i Z_i \right)^{1/2}$$

where Z_i and $\vec{x}_i$ are the atomic number and position vector of protein atom i and $\vec{m}$ is the molecular center of mass. R_G for the closed state was calculated directly from the TSAC-AK coordinates. For the open AK state, separate large and small AK domains were superimposed on the CK structure. R_G was then calculated from the AK coordinates that had been moved as rigid domains only, or after loops and subdomains had also been moved to CK-like configurations. Remodeled residues included residues 169–196 and 285–328. In the case of loop 309–319, the backbone coordinates of the aligned CK residues 315–325 were used, and no attempt was made to model the side chains. For residues 169–196 and the rest of 285–328, the AK regions were rigid-body-superimposed on the aligned Mi_bCK coordinates.

Sequence realignment

AK loop 309–319 was realigned to Mi_bCK 315–325 with a low gap penalty to allow the catalytically important AK Glu^{314} to be aligned with a similar residue, CK Asp^{321}. The ends of the β-strands to which the loop is attached are highly conserved, leading to an unambiguous alignment that was unchanged from prior reports (Dumas and Camonis, 1993; Strong, 1995). It was a nonconserved eight-residue section of the loop that was realigned. The AK and CK structures were completely different, giving no indication of how the sequences should be aligned. The prior sequence alignments could be improved by pairing Glu^{314} with Asp^{321} by inserting a gap between AK Glu^{314} and its conserved neighbor, Gly^{313}. There were seven positions in which a complementary single insertion could have been made in the CK sequence to retain the alignment in the next conserved region. The best was located by manually calculating the alignment scores of the seven possibilities, using the blosum62 comparison matrix (Henikoff and Henikoff, 1992).

Structure comparison and analysis

Coordinate differences and B-factors were analyzed using COMPAR and BAVERAGE of the CCP4 suite (Collaborative Computational Project, 1994). Interactive graphical analysis used the program O (Jones and Kjeldgaard, 1997). Structural figures were produced with MolScript (Kraulis, 1991), Raster3D (Merritt and Bacon, 1997), and GRASP (Nicholls, 1992). Accessible surface areas were calculated using MSP (Connolly, 1983). From changes in surface area, estimation of changes in the free energy of solvation followed the method of Xie and Chapman (1996), using atomic solvation parameters (Eisenberg and McLachlan, 1986) that were adjusted to account for the usual ambiguities in determining atom type from 2-Å resolution electron density.

RESULTS AND DISCUSSION

Homology and magnitude of the differences between the Mi_b-CK and AK structures

Domain orientations

If entire subunits of AK and CK are optimally superimposed as rigid bodies, the correspondence is poor: 1.7 Å for main-chain atoms. The correspondence improves substantially when the large and small domains are treated independently and when loops are excluded that are in entirely different conformations. The rms main-chain difference is then 1.0 Å for the large domain and 0.9 Å for the small domain. If the large domains of AK and CK are superimposed, then the rms main-chain difference of 4.5 Å in positions of the small domains corresponds to a 13° rotation followed by a 0.2-Å translation. The axis of rotation and other parameters of the transformation are shown in Fig. 1 and Table 1. The translational component of the motion is small (<0.25 Å; Fig. 1 and Table 1) and mostly parallel to the axis of rotation. Consistent with the x-ray scattering-based terminology of open and closed states (Forstner et al., 1996), relative to the *apo* CK structure (Fritz-Wolf et al., 1996), the domains of the AK structure (Zhou et al., 1998) are closed down upon the bound substrates. The axis of rotation passes through Pro^{100}. This is within a long extended chain connecting the two domains (that is not highly conserved), so the modest bending required could be ac-

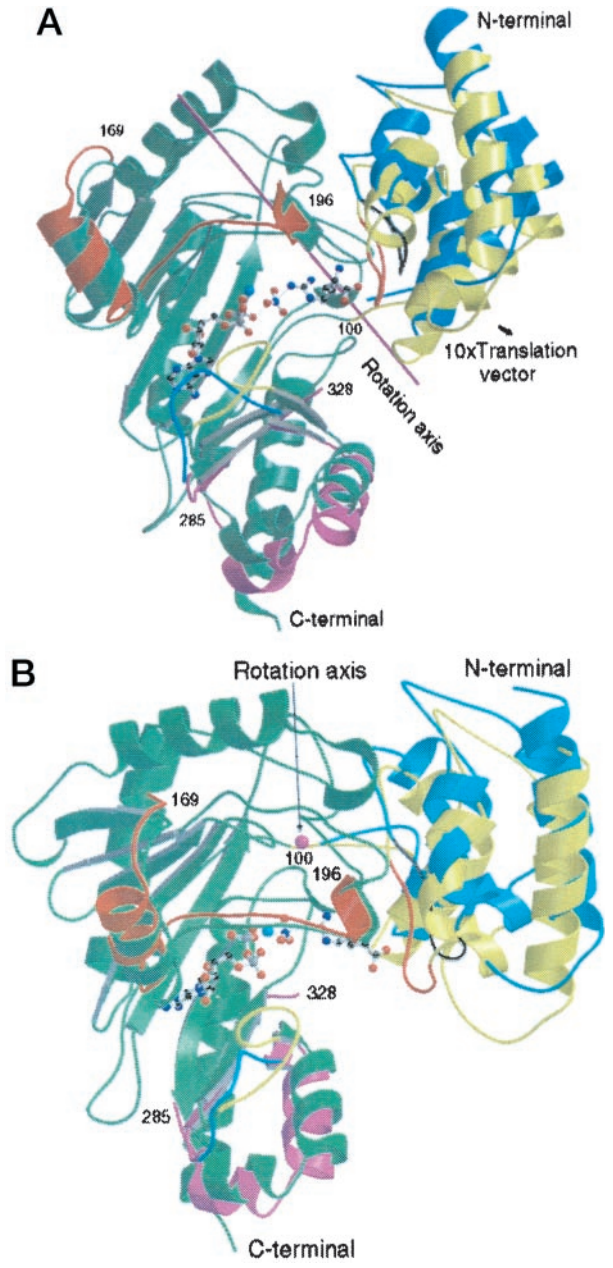

FIGURE 1 Proposed differences between the AK open and closed forms. The experimentally observed structure is shown in green (most of large domain), yellow (most of small domain and large domain loop 309–319; highlighting sites of greatest change), and red (loop 60–68). In a second model depicting the proposed substrate-free AK structure, fragments are colored cyan, black, purple, and red to highlight the regions of greatest difference: small domain in cyan/black, part of the C-terminal subdomain in cyan/purple, and region 169–196 in red. With the exception of residues 309–319, for which the corresponding actual Mi_bCK structure is shown in cyan (Fritz-Wolf et al., 1996), the apo-model consists of AK fragments that have been rigid-body superimposed on the corresponding Mi_bCK regions. Substrates are shown as ball-and-stick models. View *A* into the active site emphasizes how several loops move toward each other so that their side chains cover the substrates. View *B* is along the domain rotation axis to illustrate the hinge point and the extent of the rotation of the small domain. The Mg^{2+} is shown as a cyan sphere coordinated with the phosphates and near the center of both views.

commodated with changes to several torsion angles near Pro^{100}.

Loop conformations

There are differences in several regions, but by far the most extensive differences are in AK residues 309–319, corresponding to Mi_b-CK residues 315–325 (Figs. 2 and 3). Relative to the open-state *apo* CK, the loop of the closed-state AK is folded and twisted over the bound substrate (Figs. 2 and 4) and is very much more ordered, with an average main-chain B-factor of 11.8 $Å^2$ compared to 90.3 $Å^2$ (Table 2). The mean coordinate differences for the loop are 6.6 Å and 8.8 Å for main-chain and side atoms, respectively, showing essentially no structural correspondence. Differences for individual amino acids are listed in Table 2, but the largest is 15.0 Å for Glu^{314}, which we have aligned to Asp^{321} in CK (Table 3), based on function in the active site (Zhou et al., 1998).

Other parts of the structures differ. Loop 309–319 is part of a larger region (residues 285–328) containing a β-strand and two small α-helices that has an rms difference of 5.1 Å (Fig. 2). Another region (residues 169–196), consisting of a three-turn helix, an extended chain, and a single-turn helix, is 3.8 Å (rms) closer to the active site in the transition state analog complex. The extended chain (residues 95–115) that runs across both domains and contains the hinge point near Pro^{100} (Fig. 1) shows rms differences of 2.7 Å. With the exception of the immediate N-terminus, these are the regions in which the biggest differences occur (Fig. 3) and are the focus of this study.

Evidence that the conformational differences correspond to the substrate-induced conformational change

Crystallographic evidence of conformational changes in creatine kinase

Fritz-Wolf et al. (1996) noted several features of their Mi_b-CK structure that led them to believe that the conformations of their *apo* and ATP-bound forms would have to change to become active. The substrate positions were not fully consistent with prior spectroscopic results, active-site loops had high thermal factors, and they had different conformations in different subunits (Fritz-Wolf et al., 1996, and references therein). The sites of change required for activity predicted from the Mi_b-CK structure are entirely consistent with the sites of greatest difference with the active-state AK. The substrate nucleotide base, α and β phosphates, differ by an rms of 2.4 Å, and the *apo*-CK disordered active-site loops have a completely different configuration in AK (see above). Furthermore, except for the immediate N- and C-termini, the regions of largest conformational difference are exactly those that have the highest temperature factors in

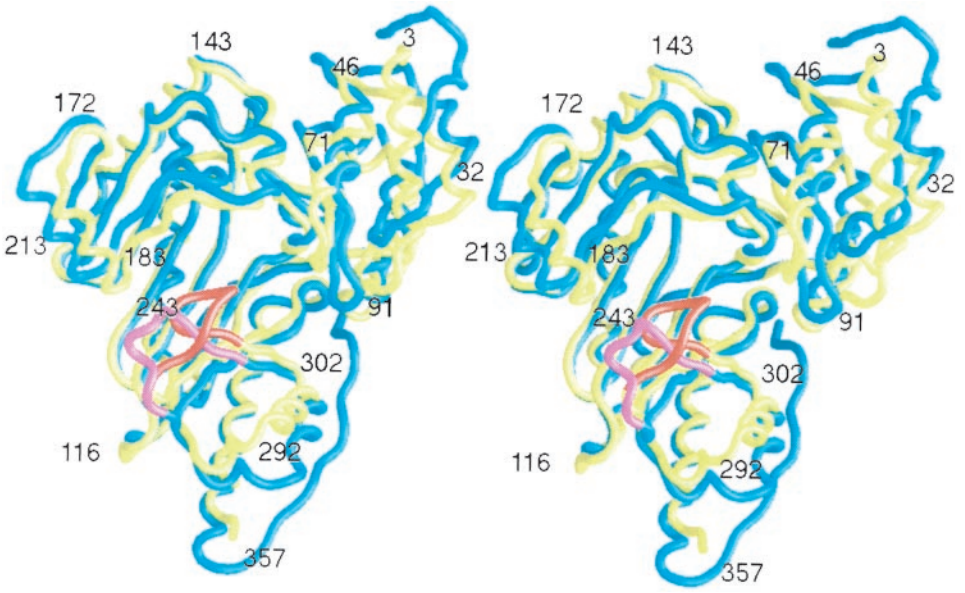

FIGURE 2 Structural differences between AK (Zhou et al., 1998) and Mib-CK (Fritz-Wolf et al., 1996). In this stereo diagram, AK is shown in yellow. Mi_b-CK (*cyan*) small and large domains were aligned independently. Loop 309–319 of AK is highlighted in red, and the corresponding CK loop 315–325 is in purple.

CK (Fig. 3), suggesting that these regions are flexible in the absence of a full complement of substrates. On a different tack, the destruction of Mi_b-CK crystals with the addition of TSA components and the failure to date of cocrystallization have also been interpreted as evidence for substantial conformational changes (Kabsch and Fritz-Wolf, 1997).

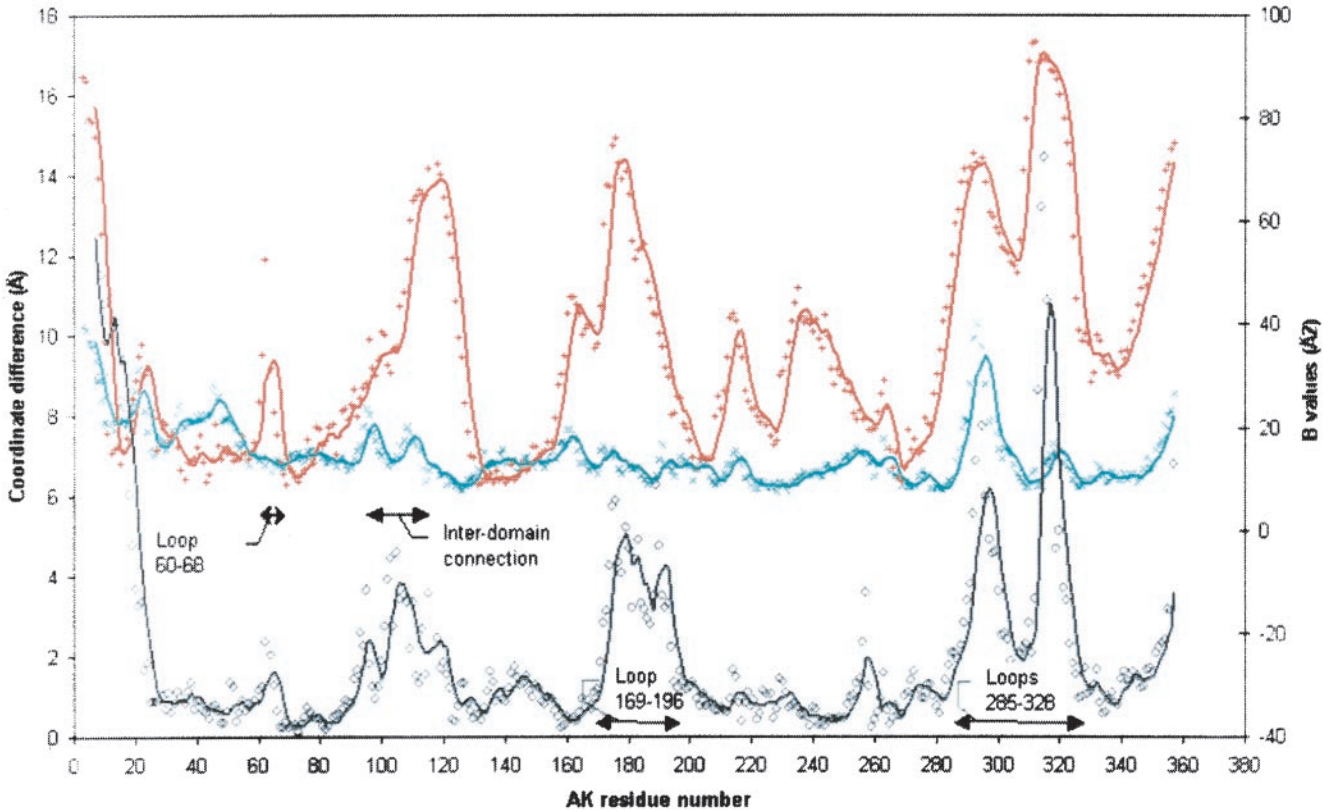

FIGURE 3 Coordinate differences and temperature factors for AK and CK after independent superimposition of the small and large domains. ○, rms main-chain differences (Å) for each residue; ×, Mean B-factors (Å^2) for AK residues; +, CK (Fritz-Wolf et al., 1996). The regions that are most involved with the conformational changes are noted; they have elevated temperature factors, indicating flexibility in (at least) the apo-form of CK.

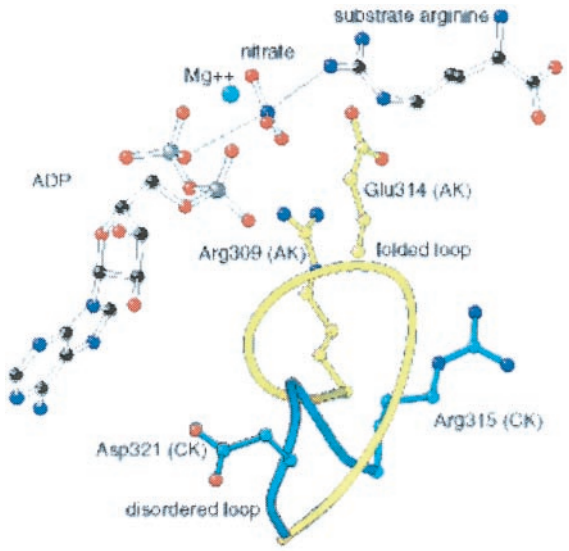

FIGURE 4 A detailed view of differences between AK loop 309–319 (*yellow*) and Mi_bCK 315–325 (*cyan*) after the large domains have been superimposed. Side chains that interact with the substrates are shown by ball-and-stick models. This figure and Fig. 1 were prepared with MOLSCRIPT (Kraulis, 1991).

Radii of gyration

The calculated radius of gyration (R_G) of the closed state AK is 20.0 Å, agreeing with values of 19.7–20.0 determined experimentally from small-angle x-ray scattering (Dumas and Janin, 1983; Forstner et al., 1998) for Mg-ATP complexes. If the AK domains are reoriented to the open-state CK positions (Fritz-Wolf et al., 1996) with a rigid domain movement, there is a predicted increase in R_G to 20.4 Å. Remodeling loops 169–196 and residues 285–328 to the obviously different backbone configurations of the open-CK structure (Fritz-Wolf et al., 1996) increases R_G to 20.8 Å. This is in reasonable agreement with experimental values of 21.2–21.5 Å (Dumas and Janin, 1983; Forstner et al., 1998). The remaining modest discrepancy between calculation and experiment may be due to subtler changes in (for example) side-chain configuration that are not obvious when comparing different enzymes, or to unrealistic assumptions in R_G calculation, such as spherical shape. Considering such factors, agreement of predicted and measured R_G is good and supports approximate modeling of open-state AK structure based on the currently known AK and CK structures.

TABLE 2 The RMS displacement and B factors of loop 309–319 in closed-state AK and the corresponding loop 315–325 in the open-state Mib-CK

Residue		⟨mean main chain B⟩ (Å^2)		RMS coordinate difference (Å)	
AK	Mi_b-CK	AK	Mi_b-CK	Main chain	Side chain
R309	R315	8.3	80.2	2.6	5.9
G310	G316	8.4	91.1	3.3	N/A
T311	T317	11.0	94.7	4.5	7.0
R312	G318	11.6	95.1	3.6	N/A
G313	G319	8.7	91.0	8.2	N/A
	V320		91.6	N/A	N/A
E314	D321	8.8	91.6	15.0	18.1
H315		13.0		N/A	N/A
T316	T322	13.3	91.6	11.1	10.6
E317	A323	14.6	89.5	6.4	4.8
S318	A324	16.9	89.0	6.4	8.0
E319	V325	15.2	87.8	5.2	7.1
Average		11.8	90.3	6.6	8.8

A B-factor of 95 Å^2 corresponds to a rms displacement of 1.1 Å from the equilibrium position.

TABLE 3 The adjusted sequence alignment of loop 315–325 (Mi_b-CK) to loop 309–319 (AK)

AK	306-LQVR	GTRG.**E**HTESEGG	VYDISN-327
Mi_b-CK	312-LQKR	GTGGV**D**.TAAVAD	VYDISN-333

Underlined segments are conserved β-sheets. AK Glu^{314}, which interacts with the substrate guanidine group, is bold, as is Mi_b-CK Asp^{321}, with which it is aligned here.

Analysis of conformational changes by comparison of different structures

Given a history of difficulties in determining the structure of the active form of CK (Kabsch and Fritz-Wolf, 1997), for the foreseeable future, the only basis for understanding the impact of conformational changes upon the mechanism of action will be through comparison of different structures. Fortunately, the approach is supported not only by the radii of gyration, but by the correlation of disorder in Mi_b-CK (Fritz-Wolf et al., 1996) with the AK-CK structural differences. Furthermore, it is not be the first time that, for practical reasons, it has been necessary to infer conformational changes by comparing structures from different species and quaternary structure. Prior examples include RuBisCO and phosphoribosyltransferases (Schreuder et al., 1993; Schumacher et al., 1996).

Significance of the conformational changes

In other enzymes, substrate-induced conformational changes have included both loop movements and domain realignments that can be either primarily rotations about a hinge point or "shear" translations (Gerstein and Krebs, 1998).

Domain movements

Analysis of the transformation shows a hinge point located at Pro^{100} with a 13° rotation about an axis roughly in the plane of the domain interface and a small 0.2-Å translation mostly parallel to the rotation axis (Fig. 1 and Table 1).

While there are some notable examples of larger hinged domain motions (e.g., adenylate kinase), the 13° AK/CK rotation is of a magnitude similar to that of most hinged motions (e.g., formate and glutamate dehydrogenases and cAMP-dependent protein kinase; Gerstein and Krebs, 1998). The hinge point is within a long stretch of extended chain, allowing domain motion with small changes in torsion angles, unhindered by secondary structure.

Loop movements

Fig. 4 highlights the loops that undergo substantial disorder-order and conformational transitions upon binding substrate and changing from open to closed forms. The loop with the greatest change (residues 309–319 in AK and 315–325 in Mi_b-CK) is also critically important in catalysis. AK-Glu^{314} binds the substrate arginine guanidinium group, holding it in precisely the right place for optimal catalysis (Zhou et al., 1998). AK-Glu^{314} is also one of two candidate bases in catalysis (Zhou et al., 1998). In prior sequence alignments (e.g., Dumas and Camonis, 1993), AK-Glu^{314} is part of an eight-residue loop segment with no sequence conservation. Based on the apparent importance of a carboxylate (Zhou et al., 1998), the alignment has been frame-shifted one amino acid with single insertions/deletions to align AK-Glu^{314} with Mib-CK-Asp^{321} (Table 3).

AK-Glu^{314} appears to be at the center of the loop motion, with the largest main-chain difference of 15.0 Å for Glu^{314}, aligned as Asp^{321} in CK (Table 3). The parallels with RuBisCO's Lys^{334} are extraordinary (Schreuder et al., 1993). Motions of an active-site loop in each exceed 12 Å; there are smaller motions or disorder-order transitions in other loops, and either domain or subunit realignments. Focusing on the active-site loop, as in RuBisCO and in contrast to triose phosphate isomerase (Joseph et al., 1990), the loop movement is more than a rigid hinged flap movement and involves the loop adopting a very different backbone conformation. In both RuBisCO and AK, salt-bridge/hydrogen bond interactions with a charged substrate group appear to lead the conformational change. In RuBisCO an enzyme lysine interacts with a substrate phosphate (Schreuder et al., 1993), and in guanidino kinases, an enzyme carboxylate interacts with a guanidinium. In both cases, the residue leading the change appears to be critical for completion of the active site and likely has a direct catalytic role.

In both RuBisCO and AK, the direct interactions of the moving loop with the substrate may ensure that the conformational change is completed only when substrate is bound. In AK, there are multiple interactions of loop 309–319 with the substrates. Arg^{309} is one of the five positively charged arginines that bind the negatively charged α and γ phosphates of ATP. With Arg^{309} interacting with the nucleotide and Glu^{314} with the substrate arginine, loop 309–319 bridges both substrates and may be partially responsible for bringing them into correct juxtaposition. Furthermore, it is only with movement of the loop (including side-chain movements of 18 and 6 Å for Glu^{314} and Arg^{309}) that the active site is configured. Like RuBisCO, HGXPRTases, and protein tyrosine phosphatase (Schreuder et al., 1993; Schumacher et al., 1996; Schubert et al., 1995), phosphagen kinases support one of Koshland's predictions (Koshland, 1958) that induced fit may initiate changes that complete the active site.

Loop 309–319 is part of a larger C-terminal region (from residue ~281 to the C-terminus) that could be considered a subdomain undergoing a plastic hinged rotation. With an axis running near residues 280 and 300, most of the subdomain is rotated ~7° toward the active site. This appears to be accomplished with small changes in the torsion angles of a number of amino acids. The region includes the three C-terminal strands of the large domain sheet. The conformational difference is accommodated by an increase in the natural twist of the sheet, with progressively larger movements from strand 4 to strand 8 of the eight-stranded sheet. The conformational changes are plastic in that there are local variations on the rigid rotation. The rigid motion accomplishes only part of the movement of loop 309–319, which also undergoes the larger nested hinged and refolding motion described above. Differences near AK residue 295 are also larger (~8 Å), with a different backbone conformation that could be as much the result of quite different AK and CK sequences as of the presence of substrates. The C-terminal helix is rigidly rotated through a smaller angle than the rest of the subdomain (5° compared to 7°), which may be due either to substrate binding or to the C-terminal membrane-associated extension present in Mi_bCK (Kabsch and Fritz-Wolf, 1997) but not AK.

The next largest difference is a near-rigid shear translation of 169–196. A two-turn helix slides ~3.8 Å over the β-sheet, and the following extended chain moves toward the active site, making some contact with the substrate nucleotide, and to other active-site loops that have changed configuration. The conformational change seems to be accommodated in a typical way (Gerstein and Krebs, 1998) by adjusted or changed side-chain rotamers in the underlying β-sheet, allowing the hydrophobic side chains of the helix to slide past. The extended chain following the helix parallels the end-to-end positions of the substrates (Fig. 1). There are a few van der Waals contacts with the substrates, but only one specific interaction, a hydrogen bond (3.0 Å) between His^{185} N_δ and the O_2' hydroxyl of the nucleotide ribose. From the same region, the C-terminal end of the two-turn helix, there is a salt bridge between Asp^{183} and Arg^{312} of the closing active-site loop. Together, these interactions may drive the conformational change. There is one more possible specific interaction between the loops that move together over the active site—a possible hydrogen bond between the side chain of Lys^{189} and the backbone carbonyl of Glu^{314}. Such interactions may help to zip the occupied active site pocket closed. They also help to reduce the solvent acces-

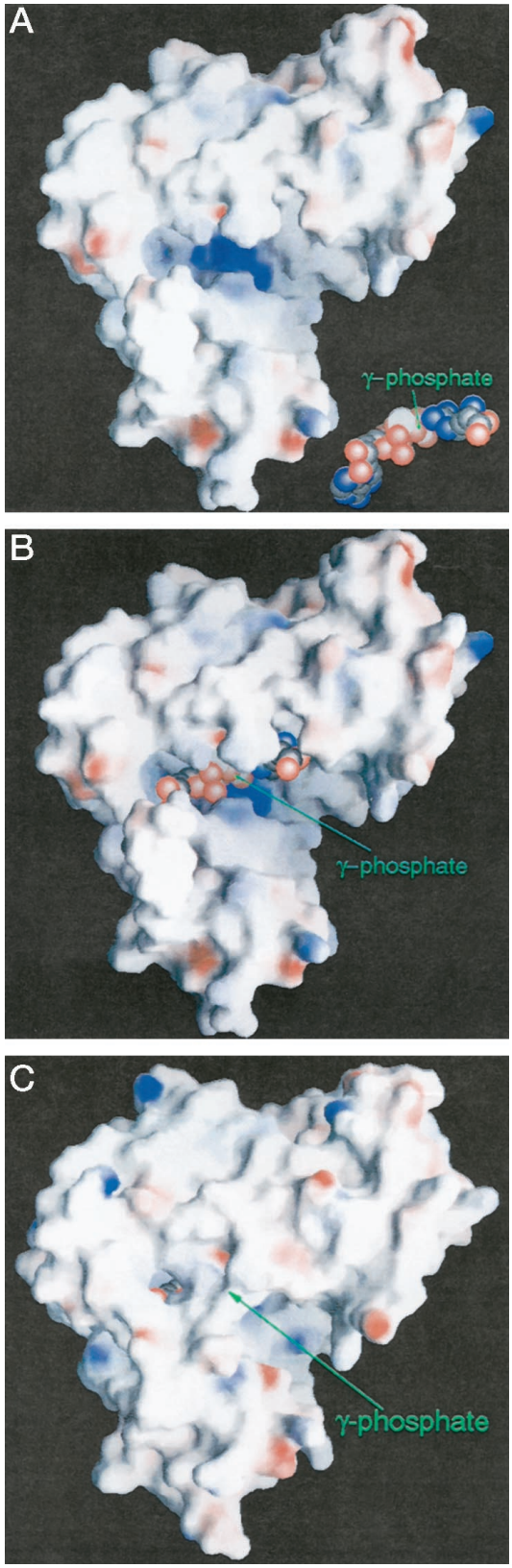

FIGURE 5 Molecular surface and electrostatic properties of the open and closed states of AK. The molecular surface of AK is shown with positive charge in blue and negative charge in red. Substrates are shown as ball-and-stick models. The location of the γ-phosphate is indicated, even if obscured by the protein. (*A*) The presumptive open state of AK based on the structure of Mib-CK. (*B*) The presumptive open state of AK with bound substrates as found in the experimentally determined closed state structure. (*C*) The closed state of AK with bound substrates. The small domain moves closer to the large domain, and loop 309–319 covers most of the substrate cavity. These figures were prepared with the program GRASP (Nicholls, 1992).

sibility. Lys^{189} restricts access to the Mg^{2+} region of the active site. The possible Lys^{189}-Glu^{314} hydrogen bond and a van der Waals interaction between the side chain of Leu^{195} and the C_δ of Glu^{225} may help to precisely position the carboxylates of Glu^{314} and Glu^{225} for their catalytic interactions with the substrate guanidinium (Zhou et al., 1998).

With crystallographic evidence of motion in Mi_bCK, Kabsch and Fritz-Wolf (1997) have predicted that regions corresponding approximately to the AK regions 309–319 and 169–196 described above might be changed in the active configuration. They also suggested that a region corresponding to AK residues 60–68 might move. It is moved closer to the active site by the rigid-body small-domain rotation, but additional local conformational differences are modest (Fig. 3). However, this loop is the site of an insertion in enzymes like CK that work upon smaller substrates (Suzuki et al., 1997b). The insertion has particularly high B-factors, which might indicate more extensive motion in CK (Fritz-Wolf et al., 1996) than AK.

Entrance to the active site

The molecular surface and electrostatic properties of the presumed open and closed state structures of AK are shown in Fig. 5. In the open state, the active site is wide open, and there is a region of strong positive charge that will bind the negatively charged ATP phosphates. With substrate bound, but with the open enzyme configuration, the accessible surface area of the γ-phosphate is ~10 $Å^2$. With the change to the closed state, the γ-phosphate is covered and becomes completely inaccessible to solvent. Thus, as in some other kinases (Anderson et al., 1979, and see below), one of the effects of the conformational change is to exclude water and reduce the chance of wasteful hydrolytic loss of ATP. By both configuring the catalytic elements and simultaneously excluding solvent with a substrate-induced conformational change, the enzyme appears to ensure that all ATP is used for productive phosphoryl transfer. Closing of the enzyme active site is mostly due to the folding down of a "flap" made by loop 309–319, but there are also contributions from the domain movement and the movement of region 169 to 196.

Potential impact of conformational differences upon quaternary structure

Horseshoe crab AK does not form octamers as does Mi_bCK. One of the Mi_bCK interdimer contact points identified by Kabsch and Fritz-Wolf (1997) contains Mi_bCK W264, which is known to affect octamer dissociation (Gross and Wallimann, 1995; Gross et al., 1994), that is present only in octameric CKs, and is within a region deleted from the AK sequence (MibCK residues 260–264). Differences between the *apo*-CK and TSAC-AK structures provide a rationale for octamer dissociation in Mi_bCK. The second interdimer contact point is at the N-terminus (Kabsch and Fritz-Wolf, 1997). Considering only a rigid small domain reorientation, the N-terminal contact region (which is far from the rotation axis) would move more than 6 Å, widening the separation of the contact points and perhaps straining the octamer interactions.

Biological implications and conclusion

The phosphagen or guanidino kinases catalyze the buffering of cellular ATP levels through the reversible transfer of the γ-phosphoryl between ATP and a guanidino substrate (Wallimann et al., 1992). They constitute one of the most intensively studied enzyme families (Stroud, 1996). Our comparison of the substrate-bound transition-state complex structure of arginine kinase (Zhou et al., 1998) with that of *apo*-creatine kinase (Fritz-Wolf et al., 1996) indicates that large conformational changes accompany substrate binding.

Role of the conformational changes

Movement of the 309–319 loop brings catalytic residues (e.g., E314) into contact with the reactive substrate groups. This component of the induced fit may minimize wasteful ATP hydrolysis by configuring the active site only when the appropriate specific substrates are present (Koshland, 1958). What about the domain movements and other changes? Rationales of induced fit proposed for other enzymes (e.g., Anderson et al., 1979) are likely to be relevant here. Solvent accessibility of the substrates is substantially reduced (Fig. 5), further reducing wasteful ATP hydrolysis and reducing the dielectric. As in hexokinase (Anderson et al., 1979) and adenylate kinase (Pai et al., 1977), a low dielectric likely enhances the nucleophilicity of the phosphoryl acceptor and increases the pK of potential carboxylate catalytic bases (E225 and E314; Zhou et al., 1998). Likely associated with the conformational changes is the sharp contrast between the disordered ADP and active-site loops of the open-form Mi_bCK binary complex (Fritz-Wolf et al., 1996) and the low B-factors of substrates and active site in the AK transition-state analog complex (Zhou et al., 1998). It appears that the folding of loop 309–319, the rotations of the small domain and C-terminal subdomain, and the shearing motion of 169–196 together envelop the substrates, fixing them in catalytically optimal positions with lower entropy. Substrate alignment is precise enough (Zhou et al., 1998) that it could be a significant part of the catalytic enhancement of rate (Dafforn and Koshland, 1971; Jencks and Mage, 1974). The participation of induced fit changes in catalysis may prove to be more generally applicable as more transition state structures of multimolecular enzyme reactions become available.

We thank Wolfgang Kabsch for access to CK atomic coordinates before data base release; Golapakrishnan Parthasarathy, Scott Strong, Thayumanasamy Somasundaram, and Eric Blanc for participation in earlier parts of the structure determination; and Thayumanasamy Somasundaram for help in producing figures.

We gratefully acknowledge the National Science Foundation for support of methods development that allowed structure determination (MSC; BIR94-18741), and the American Heart Association, Florida Division (MSC; 9701728), the National Institutes of Health (MSC; 1R29GM55837), the National Science Foundation (WRE; IBN96-31907), and the Lucille P. Markey Charitable Trust for support of evolutionary and structural studies of arginine kinase.

Coordinates and structure factors for the arginine kinase transition state analog complex have been deposited with the Protein Data Bank (entry 1bg0).

REFERENCES

Alber, T. C., R. C. Davenport, D. A. Giammona, E. Lolis, G. A. Petsko, and D. Ringe. 1987. Crystallography and site-directed mutagenesis of yeast triosephosphate isomerase: what can we learn and catalysis from a "simple" enzyme. *Cold Spring Harb. Symp. Quant. Biol.* 52:603–613.

Anderson, C. M., F. H. Zucker, and T. A. Steitz. 1979. Space-Filling Models of Kinase Clefts and Conformation Changes. *Science.* 204: 375–380.

Babbitt, P. C., G. L. Kenyon, I. D. Kuntz, F. E. Cohen, J. D. Baxter, P. A. Benfield, J. D. Buskin, W. A. Gilbert, S. D. Hauschka, J. P. Hossle, C. P. Ordahl, M. L. Pearson, J.-C. Perriard, L. A. Pickering, S. D. Putney, B. L. West, and R. A. Ziven. 1986. Comparisons of creatine kinase primary structures. *J. Protein Chem.* 5:1–14.

Bennett, W. S., Jr., and T. A. Steitz. 1980. Structure of a complex between yeast hexokinase A and glucose II. Detailed comparisons of conformation and active site configuration with the native hexokinase B monomer and dimer. *J. Mol. Biol.* 140:211–230.

Blethen, S. L. 1972. Kinetic properties of the arginine kinase isoenzymes of *Limulus polyphemus. Arch. Biochem. Biophys.* 149:244–251.

Boyer, R. 1998. Concepts in Biochemistry. Brooks/Cole, Pacific Grove, CA.

Collaborative Computational Project N. 1994. The CCP4 Suite: Programs for Protein Crystallography. *Acta Crystallogr.* D50:760–763.

Connolly, M. L. 1983. Solvent accessible surfaces of proteins and nucleic acids. *Science.* 221:709–713 .

Dafforn, A., and D. E. Koshland, Jr. 1971. Theoretical aspects of orbital steering. *Proc. Natl. Acad. Sci. USA.* 68:2463–2467.

Dumas, C., and J. Camonis. 1993. Cloning and sequence analysis of the cDNA for arginine kinase of lobster muscle. *J. Biol. Chem.* 268: 21599–21606.

Dumas, C., and J. Janin. 1983. Conformational changes in arginine kinase upon ligand binding seen by small-angle x-ray scattering. *FEBS Lett.* 153:128–130.

Eisenberg, D., and A. D. McLachlan. 1986. Solvation energy in protein folding and binding. *Nature.* 319:199–203.

Fersht, A. 1985. Enzyme Structure and Function. Freeman, New York.

Forstner, M., M. Kriechbaum, M. P. Laggner, and T. Wallimann. 1996. Changes of creatine kinase structure upon ligand binding as seen by small-angle scattering. *J. Mol. Struct.* 383:217–227.

Forstner, M., K. Manfred, P. Laggner, and T. Wallimann. 1998. Structural changes of creatine kinase upon substrate binding. *Biophys. J.* 75: 1016–1023.

Fritz-Wolf, K., T. Schnyder, T. Wallimann, and W. Kabsch. 1996. Structure of mitochondrial creatine kinase. *Nature.* 381:341–345.

Gerstein, M., and C. Chothia. 1991. Analysis of protein loop closure. Two types of hinges produce one motion in lactate dehydrogenase. *J. Mol. Biol.* 220:133–149.

Gerstein, M., and M. Krebs. 1998. A database of macromolecular motions. *Nucleic Acids Res.* 26:4280–4290.

Gerstein, M., A. M. Lesk, and C. Chothia. 1994. Structural mechanisms for domain movements in proteins. *Biochemistry.* 33:6739–49.

Gross, M., E. M. Furter-Graves, T. Wallimann, H. M. Eppenberger, and R. Furter. 1994. The tryptophan residues of mitochondrial creatine kinase: roles of Trp-223, Trp-206, and Trp-264 in active-site and quaternary structure formation. *Protein Sci.* 3:1058–1068.

Gross, M., and T. Wallimann. 1995. Dimer-dimer interaction in octameric mitochondrial creatine kinase. *Biochemistry.* 34:6660–6667.

Hansen, D. E., and J. R. Knowles. 1981. The stereochemical course of the reaction catalyzed by creatine kinase. *J. Biol. Chem.* 256:5967–5969.

Henikoff, S., and J. G. Henikoff. 1992. Amino acid substitution matrices from protein blocks. *Proc. Natl. Acad. Sci. USA.* 89:10915–10919.

Jencks, W. P., and M. I. Mage. 1974. "Orbital steering," entropy and rate accelerations. *Biochem. Biophys. Res. Commun.* 57:887–892.

Jones, T. A., and M. Kjeldgaard. 1997. Electron-density map interpretation. *Methods Enzymol.* 277:173–208.

Joseph, D., G. A. Petsko, and M. Karplus. 1990. Anatomy of a conformational change: hinged "lid" motion of the triosephosphate isomerase loop. *Science.* 249:1425–1428.

Kabsch, W. 1976. A solution for the best rotation to relate two sets of vectors. *Acta Crystallogr. A.* 32:922–923.

Kabsch, W., and K. Fritz-Wolf. 1997. Mitochondrial creatine kinase—a square protein. *Curr. Opin. Struct. Biol.* 7:811–818.

Kenyon, G. L., and G. H. Reed. 1983. Creatine kinase: structure-activity relationships. *Adv. Enzymol.* 54:367–426.

Koshland, D. E. J. 1958. Application of a theory of enzyme specificity to protein synthesis. *Proc. Natl. Acad. Sci. USA.* 44:98–104.

Kraulis, P. 1991. MOLSCRIPT: a program to produce both detailed and schematic plots of protein structures. *J. Appl. Crystallogr.* 24:946–950.

Lui, N. S. T., and L. Cunningham. 1966. Cooperative effects of substrates and substrate analogs on the conformation of creatine phosphokinase. *Biochemistry.* 5:144–149.

McDonald, R. C., T. A. Steitz, and D. M. Engelman. 1979. Yeast hexokinase in solution exhibits a large conformational change upon binding glucose or glucose 6-phosphate. *Biochemistry.* 18:338–342.

Merritt, E. A., and D. J. Bacon. 1997. Raster3D: photorealistic molecular graphics. *Methods Enzymol.* 277:505–525.

Mühlebach, S., M. Gross, T. Wirz, T. Wallimann, J. C. Perriard, and M. Wyss. 1994. Sequence homology and structure predictions of the creatine kinase isoenzymes. *Mol. Cell Biochem.* 133/4:245–262.

Nicholls, A. 1992. GRASP: Graphical Representation and Analysis of Surface Properties. Columbia University, New York.

Page, M. I., and W. P. Jencks. 1971. Entropic contributions to rate accelerations in enzymic and intramolecular reactions and the chelate effect. *Proc. Natl. Acad. Sci. USA.* 68:1678–1683.

Pai, E. F., W. Sachsenheimer, R. H. Schirmer, and G. E. Schulz. 1977. Substrate positions and induced-fit in crystalline adenylate kinase. *J. Mol. Biol.* 114:37–45.

Rao, J. K., G. Bujacz, and A. Wlodawer. 1998. Crystal structure of rabbit muscle creatine kinase. *FEBS Lett.* 439:133–137.

Rao, B. D. N., D. H. Buttlaire, and M. Cohn. 1976. ^{31}P NMR studies of the arginine kinase reaction. *J. Biol. Chem.* 251:6981–6986.

Reed, G. H., and M. Cohn. 1972. Structural changes induced by substrates and anions at the active site of creatine kinase. *J. Biol. Chem.* 247: 3073–3081.

Rhee, S., K. D. Parris, C. C. Hyde, S. A. Ahmed, E. W. Miles, and D. R. Davies. 1997. Crystal structures of a mutant (betaK87T) tryptophan synthase alpha2beta2 complex with ligands bound to the active sites of the alpha- and beta-subunits reveal ligand-induced conformational changes. *Biochemistry.* 36:7664–7680.

Rojo, M., R. Hovius, R. A. Demel, K. Nicolay, and T. Wallimann. 1991. Mitochondrial creatine kinase mediates contact formation between mitochondrial membranes. *J. Biol. Chem.* 266:20290–20295.

Schreuder, H. A., S. Knight, P. Curmi, I. Andersson, D. Cascio, C.-I. Brändén, and D. S. Eisenberg. 1993. Formation of the active site of ribulose-1,5-bisphosphate carboxylase/oxygenase by a disorder-order transition from the unactivated to the activated form. *Proc. Natl. Acad. Sci. USA.* 90:9968–9972.

Schubert, H. L., E. B. Fauman, J. A. Stuckey, J. E. Dixon, and M. A. Saper. 1995. A ligand-induced conformational change in the Yersinia protein tyrosine phosphatase. *Protein Sci.* 4:1904–1913.

Schumacher, M. A., D. Carter, D. S. Roos, B. Ullman, and R. G. Brennan. 1996. Crystal structures of *Toxoplasma gondii* HGXPRTase reveal the catalytic role of a long flexible loop. *Nature Struct. Biol.* 3:881–887.

Stein, H. D., D. A. Harn, and J. R. David. 1990. A cloned ATP:guanidino kinase in the trematode *Schistosoma mansoni* has a novel duplicated structure. *J. Biol. Chem.* 265:6582–6588.

Strong, S. 1995. Molecular studies of arginine kinase isoforms. Ph.D. dissertation. Florida State University, Tallahassee.

Strong, S. J., and W. R. Ellington. 1993. Horseshoe crab sperm contain a unique isoform of arginine kinase that is present in midpiece and flagellum. *J. Exp. Zool.* 267:563–571.

Strong, S. J., and W. R. Ellington. 1995. Isolation and sequence analysis of the gene for arginine kinase from the chelicerate arthropod, *Limulus polyphemus*: insights into catalytically important residues. *Biochim. Biophys. Acta.* 1246:197–200.

Stroud, R. M. 1996. Balancing ATP in the cell. *Nature Struct. Biol.* 3:567–569.

Suzuki, T., and T. Furukohri. 1994. Evolution of phosphagen kinase: primary structure of glycocyamine kinase and arginine kinase from invertebrates. *J. Mol. Biol.* 237:353–357.

Suzuki, T., Y. Kawasaki, and T. Furukohri. 1997a. Evolution of phosphagen kinase. Isolation, characterization and cDNA-derived amino acid sequence of two-domain arginine kinase from the sea anemone *Anthopleura japonicus. Biochem. J.* 328:301–306.

Suzuki, T., Y. Kawasaki, T. Furukohri, and W. R. Ellington. 1997b. Evolution of phosphagen kinase. VI. Isolation, characterization and cDNA-derived amino acid sequence of lombricine kinase and the earthworm *Eisenia foetida*, and identification of a possible candidate for the guanidine substrate recognition site. *Biochim. Biophys. Acta.* 1343: 152–159.

Wallimann, T., M. Wyss, D. Brdiczka, K. Nicolay, and H. M. Eppenberger. 1992. Intracellular compartmentation, structure and function of creatine kinase isoenzymes: the "phospho-creatine circuit" for cellular energy homeostasis. *Biochem. J.* 281:21–40.

Wothe, D. D., H. Charbonneau, and B. M. Shapiro. 1990. The phosphocreatine shuttle of sea urchin sperm: flagellar creatine kinase resulted from a gene triplication. *Proc. Natl. Acad. Sci. USA.* 87:5203–5207.

Wyss, M., J. Smeitink, R. A. Wevers, and T. Wallimann. 1992. Mitochondrial creatine kinase: localization, structure and function, and clinical aspects. *Biochim. Biophys. Acta.* 288:771–775.

Xie, Q., and M. S. Chapman. 1996. Canine parvovirus capsid structure, analyzed at 2.9 Å resolution. *J. Mol. Biol.* 264:497–520.

Zhou, G., T. Somasundaram, E. Blanc, Z. Chen, and M. S. Chapman. 1999. Critical initial real-space refinement in the structure determination of arginine kinase. *Acta Crystallogr. D Biol. Crystallogr.* 55:835–845.

Zhou, G., T. Somasundaram, E. Blanc, G. Parthsarathy, W. R. Ellington, and M. S. Chapman. 1998. Transition state structure of arginine kinase: implications for catalysis of bimolecular reactions. *Proc. Natl. Acad. Sci. USA.* 95:8449–8454.